

Lifetime of excitons localized in Si nanocrystals in amorphous silicon

© O.B. Gusev*, A.V. Belolipetskiy*, I.N. Yassievich*, A.V. Kukin⁺, E.E. Terukova⁺, E.I. Terukov⁺

* Ioffe Institute,

194021 St. Petersburg, Russia

⁺ R&D Center of thin-film technology for energetics under Ioffe Physicotechnical Institute,

194021 St. Petersburg, Russia

E-mail: alexey.belolipetskiy@mail.ioffe.ru

(Получена 1 октября 2015 г. Принята к печати 6 октября 2015 г.)

The introduction of nanocrystals plays an important role in improving the stability of the amorphous silicon films and increasing the carrier mobility. Here we report results of the study on the photoluminescence and its dynamics in the films of amorphous hydrogenated silicon containing less than 10% of silicon nanocrystals. The comparing of the obtained experimental results with the calculated probability of the resonant tunneling of the excitons localized in silicon nanocrystals is presented. Thus, it has been estimated that the short lifetime of excitons localized in Si nanocrystal is controlled by the resonant tunneling to the nearest tail state of the amorphous matrix.

1. Introduction

Amorphous hydrogenated silicon (*a*-Si:H) is one of the principal materials in manufacturing low-cost thin-film solar cells. The main drawback of the amorphous silicon is its photoinduced degradation (Staebler–Wronski effect) [1]. Recently, nanostructured films of nanocrystalline silicon imbedded in amorphous hydrogenated silicon matrix received much attention [2–5]. It has been shown that stability and efficiency of solar cells can be dramatically increased by using an intrinsic layer and/or a high conduction doped layer of *a*-Si:H where the volume fraction of Si nanocrystals exceeds 30%.

Here we report the results of the study on the photoluminescence (PL) and PL kinetics of the films of amorphous hydrogenated silicon containing silicon nanocrystals (less than 10%) in a wide spectral range. The goal of the investigation was to elucidate PL relaxation mechanism. This research is also interesting from the fundamental viewpoint since we are studying a material where nanocrystals form quantum dots for the carriers on the background of the tail states of the amorphous matrix.

2. Sample preparation and experimental details

Films of *a*-Si:H (thickness, 170 nm) with nanocrystalline inclusions were obtained by decomposition of silane (SiH₄) diluted with hydrogen on the setup for plasma chemical deposition KAI-1200 manufactured by TEL Solar (former Oerlikon Solar). Our experiments have shown that conditions necessary for the preparation of *a*-Si:H with nanocrystalline inclusions lay in a rather narrow range. In our case the operating pressure has been on the level of 2.4 mbar, the gases ratio in the reactor chamber has been $R_H = [H_2]/[SiH_4] = 31$ at the discharge power of 1200 W. The films have been deposited on the glass and silicon substrate at 200°C with deposition rate 4 Å/s.

The stationary PL has been excited by the semiconductor laser emitting at $\lambda = 405$ nm and has been registered with a photomultiplier or with a cooled germanium receiver. The time-resolved PL spectra have been obtained at the excitation with a pulse nitrogen laser emitting at $\lambda = 337$ nm with the pulses 10 ns long at the repetition frequency of 180 Hz. The PL measurements have been carried out using a grating monochromator, a stroboscopic voltage converter with the strobe (width 4 nm) and a digital oscilloscope. The time resolution of the registration system at the use of photomultiplier has been 10 ns in the spectral interval 400–900 nm.

The spectra and the kinetics of PL decay have been studied at room temperature and at 77 K on the films deposited on quartz substrate. In experiments at 77 K the samples have been directly submerged in the liquid nitrogen. All PL spectra are reported taking in consideration the spectral sensitivity of the optical system.

3. Experimental results

In Fig. 1 PL spectra are presented for a film of *a*-Si:H with silicon nanocrystals (Si NCs) deposited at the pressure of 2.4 mbar. The measurements were carried out at room temperature at stationary (Fig. 1, *a*) and pulse (Fig. 1, *b*) excitation modes.

At the stationary excitation (Fig. 1, *a*) two PL bands are observed with maxima at 543 and 615 nm. We believe that these bands originate from silicon nanocrystals located in the oxidized surface layer of the *a*-Si:H film. In correspondence to the literature data the size of nanocrystals can be estimated to be around 1.5 and 2 nm, respectively. As seen from Fig. 1, *b*, these bands shifted to the blue region appear also at the pulse excitation on the background of wide PL band characteristic of silicon suboxide. As known, the PL from the tail states of the *a*-Si:H matrix is not observed at the room temperature [6]. We believe that the PL band in the region of 800 nm, observed both at the stationary and pulse excitation at room temperature,

results from the emission of silicon nanocrystals located in the depth of the *a*-Si:H film. At the pulse photoexcitation this band is considerably more intense than at the stationary mode, in contrast to the emission from the nanocrystals located near the surface (bands with the maxima at 615 and 543 nm), and it possesses a pronounced maximum at 780 nm (1.6 eV). Thus, the experiment shows the short lifetime of excitons localized in the silicon nanocrystals situated in an amorphous matrix.

Fig. 2 shows the PL spectrum of the *a*-Si:H film with Si NCs registered at 77 K at the pulse excitation $\lambda = 355$ nm. In the insert of Fig. 2, the PL kinetics is demonstrated for three different wavelengths. As seen from the figure, for all three PL values corresponding to 750, 770, and 800 nm the PL decay is characterized by two components, first with decay time less than 10 ns and, second with decay time of the order of 100 ns. It is natural to assume that the slow component of the PL decay is due to the radiative transitions between the tail states of the conduction and the valence bands.

The spectral distribution and the kinetics of the photoluminescence band originated from the recombination

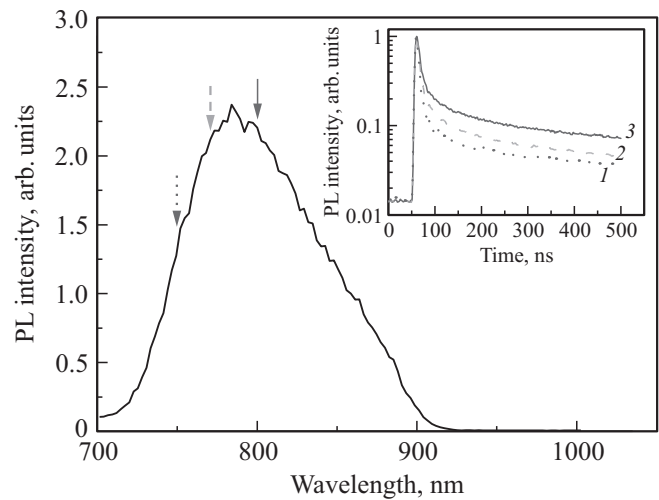


Figure 2. PL spectrum of *a*-Si:H with Si NCs. $T = 77$ K. On insert: PL decay at 750 nm (1.65 eV) (1), 770 nm (1.61 eV) (2), and 800 nm (1.55 eV) (3).

between the tail states in the pure *a*-Si:H were thoroughly studied [6]. This wide luminescence band is absent at the room temperature but is well seen at 77 K with a peak at 900 nm (1.37 eV) and is characterized by the decay time of the order of ms.

The photoluminescence of the silicon nanocrystals in our sample appears on the background of this band, but it is characterized by a much faster component with the decay time of less than 10 ns. The spectrum shown in this figure was registered using photomultiplier, therefore the long wavelength part over 900 nm was absent.

4. Theory and discussion

We studied spectra and PL kinetics for several *a*-Si:H films prepared at the pressure in the range 2–3 mbar. It turned out that characteristically spectra of all samples contained two bands with the maxima in the region 600 and 800 nm, corresponding to the luminescence of the nanocrystals from the oxidized surface layer and from the bulk of the amorphous silicon, respectively.

Let us estimate the radiative lifetime of an electron-hole pair in the silicon nanocrystal located in the matrix of the amorphous silicon. The rate of the radiative recombination of exciton in the nanocrystal depends on the refraction index of the environment [7]:

$$\frac{1}{\tau_{\text{rad}}} \propto F^2 n_{\text{out}}, \tag{1}$$

where $F = 3n_{\text{out}}^2 / (n_{\text{in}}^2 + n_{\text{out}}^2)$, n_{in} and n_{out} are refractive indices inside and outside of the nanocrystal, respectively. At a low density of the nanocrystals for the nanocrystals in the oxidized layer $n_{\text{out}} = 1.4$ (refractive index of SiO₂), and for the nanocrystals in the matrix of the amorphous silicon $n_{\text{out}} = 3.4$ (refractive index of *a*-Si:H), practically the same

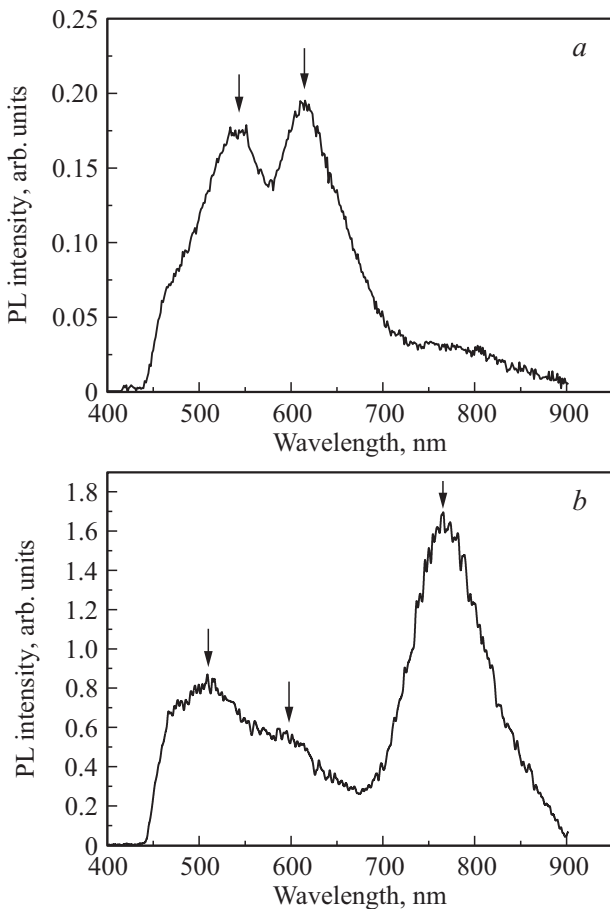


Figure 1. PL spectra from a film of *a*-Si:H with silicon nanocrystals deposited at the pressure of 2.4 mbar at the stationary (a) and pulse (b) excitation. Measurements were performed at room temperature.

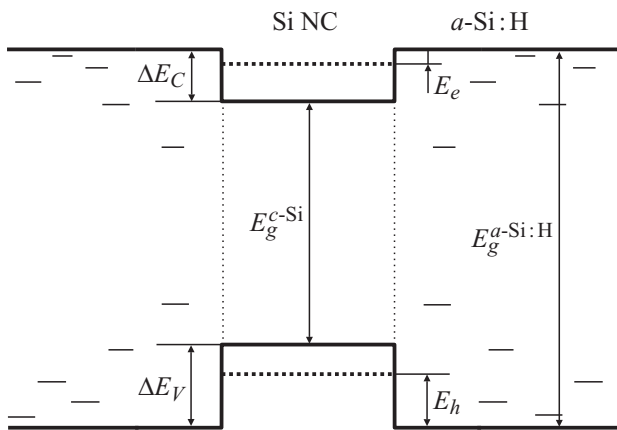


Figure 3. Energy band diagram of the *a*-Si:H containing silicon nanocrystals. Band offsets ΔE_C and ΔE_V for electrons and holes at the Si/*a*-Si:H boundary are shown. Dotted lines correspond to the energy levels of the carriers localized in Si NC. Short dashes demonstrate the existence of local energy levels generated by potential fluctuations in *a*-Si:H.

value as the silicon refractive index. From expression (1) we expect that the radiative lifetime of the nanocrystals in the matrix of the *a*-Si:H should be about 20 times less than in the oxidized SiO₂ layer at the same dimensions. The radiative lifetime of excitons in silicon nanocrystals in silicon dioxide depending on size occurs in the time interval from $3 \cdot 10^{-5}$ s to 10^{-3} s (see, e.g., [8,9]). Therefore, even for the smallest nanocrystals in *a*-Si:H the expected radiative lifetime should not be shorter than 1μ s. The observed fast photoluminescence decay shows, that the lifetime of excitons in the silicon nanocrystals in the *a*-Si:H matrix is less than 10 ns. Thus this short lifetime is due to a nonradiative process. As we show further, it is originated from a tunnel transition of localized carriers to the tail states of the amorphous matrix.

The photoluminescence of silicon nanocrystals occurs by the radiative recombination of a localized electron-hole pair, i.e., localized exciton. Excitons, localized in nanocrystals, are formed due to capturing of the carriers appearing in the matrix, as a result of the light absorption. The energy zone diagram of the *a*-Si:H containing silicon nanocrystals is shown in Fig. 3.

In the calculation of the ground levels of Si NCs in the *a*-Si:H matrix we used the method of effective mass. As effective masses of electron and hole in Si NCs and in the *a*-Si:H matrix we used the density states effective masses of bulk silicon, namely, $m_e = 0.33m_0$ for electrons and $m_h = 0.5m_0$ for holes, m_0 being the free electron mass. Usually, the energy of the order of 1.80–1.85 eV is taken as the forbidden gap E_g for *a*-Si:H, which determines the energy gap between the carrier mobility edges in the conduction and the valence bands. We analyze the experimental results by comparing them with the calculations carried out in [10], where the value $E_g = 1.82$ eV has been used. The value

$\Delta E_V = 0.4$ eV for the valence band offset at the Si/*a*-Si:H boundary (see Fig. 3) has been found experimentally [11]. Consequently, the value $\Delta E_C = 0.25$ eV should be used for the conduction band offset.

The band offset and the effective mass for holes is larger than that for electrons; as a result, the energy of the hole localization in the ground state is considerably larger. As shown in [10] this leads to the formation of an exciton by initially capturing a hole into the nanocrystal and later an electron. In this case the additional electrostatic potential generated by the localized hole plays an essential role in the effective potential for electron localization. The calculation results of the energy of the localized exciton as function of the NC size are presented in Fig. 4. The localization energies of the hole and the electron in the exciton state are shown in the insert.

There are tails of the density of states for electrons and holes in the effective forbidden gap in *a*-Si:H. The carriers localized in Si NCs can undergo tunneling from the nanocrystals to the tail states. The most probable is the resonant tunneling to the nearest tail state which energy coincides with the energy of the localized carrier. The probability of such processes calculated in [10] for holes and electrons that accounts for the Coulomb attraction by the captured hole, is presented as a function of the nanocrystal size in Fig. 5.

As seen from Fig. 5, the tunneling probabilities of holes and electrons are close to each other for the nanocrystals of all sizes and they decrease exponentially with the growing dimensions of the nanocrystals. This is due to the exponential decrease in the density of the tail states with the growing localization energy.

The calculated probabilities of the resonant tunneling determine the lifetime of the exciton in the nanocrystal if the carrier appearing in the tail state would rather go over to the

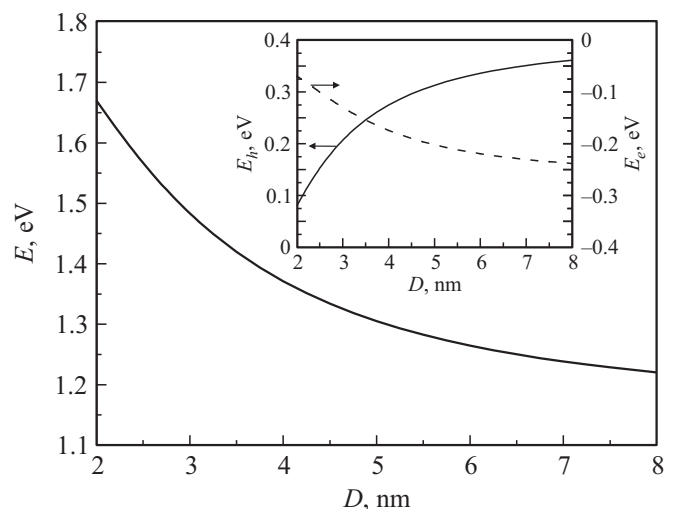


Figure 4. Dependence of PL band energy of nanocrystals in the *a*-Si:H matrix on the nanocrystal diameter D . The localization energies of the hole and the electron in the exciton state are shown in the insert according to the data of [10].

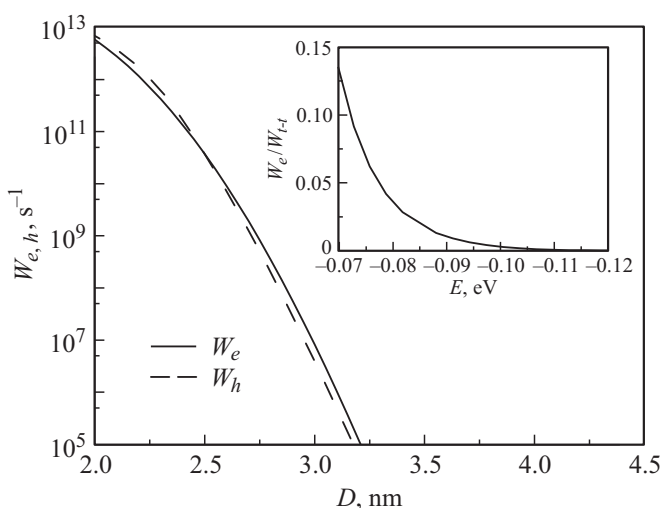


Figure 5. Probabilities $W_{e,h}$ of the resonant tunneling of holes and electrons from nanocrystals to the nearest tail state as functions of the nanocrystal diameter D . Insert: the ratio of the probability of the resonant tunneling of electron to the nearest tail state to the probability of its tunneling between the nearest tail states as a function of the electron localization energy E .

other tail state than moving return back to the nanocrystal. The probabilities of the reverse and direct tunnel transitions are close. We calculated the probability of the resonant tunnel transition between two adjacent tail states as a function of the localization energy in accordance with [10]. It turned out that for holes the probability of the tunneling between two tail states is more than tenfold higher than the probability of tunneling from the nanocrystal, whereas for electron these probabilities are comparable. In the insert of Fig. 5, we demonstrated the ratio of the probability of the resonant tunneling of an electron confined in NC to the nearest tail state (W_e) to the probability of its tunneling between the nearest tail states (W_{t-t}) as a function of the electron localization energy. As can be seen, this ratio is $W_e/W_{t-t} < 1$. Therefore, the nonradiative lifetime of the exciton in the nanocrystal actually is governed by the probability of the resonant tunneling of carriers from the nanocrystal to the tail states. The calculated lifetimes of electrons and holes localized in Si NCs sharply decrease with reducing the size of the nanocrystals from $0.1 \mu\text{s}$ for Si NCs with sizes about 3 nm to 0.2ps for Si NCs with sizes about 2 nm.

The decay kinetics have been measured (see Fig. 2) at the photoluminescence energies corresponding to the exciton energies for the Si NCs of sizes in the range of 2.1–2.6 nm (Fig. 4). As seen from the insert in Fig. 3, for the largest nanocrystals (2.6 nm) the short decay time less than 10 ns is in agreement with the calculated lifetime determined by resonant tunneling (see Fig. 5). For smaller nanocrystals the decay time is essentially shorter as should be expected. Consequently, the observed PL intensity also decreases. The electron microscopy shows that in the film under study

the majority of nanocrystals is smaller than 2 nm. Due to the short lifetime of exciton in these nanocrystals their contribution to PL is ineffective.

5. Conclusion

In conclusion, the short exciton lifetime of the order of 10 ns, which has been observed in the nanostructured amorphous silicon film, is controlled by resonant tunneling of the carriers localized in silicon nanocrystals to the nearest tail states of the amorphous matrix.

Acknowledgments: The study has been partially supported by the Russian Foundation for Basic Research (grants 14-02-00119, 15-02-09034, and 13-02-00017).

References

- [1] D.L. Staebler, C.R. Wronski. *Appl. Phys. Lett.*, **31**, 292 (1977).
- [2] Guozhen Yue, Baojie Yan, Gautam Ganguly, Jeffrey Yang, Subhendu Guha, Charles W. Teplin. *Appl. Phys. Lett.*, **88**, 263 507 (2006).
- [3] Keda Wang, Daxing Han, Guozhen Yue, Baojie Yan, Jeffrey Yang, Subhendu Guha. *Appl. Phys. Lett.*, **95**, 023 506 (2009).
- [4] K.G. Kiriluk, J.D. Fields, B.J. Simonds, Y.P. Pai, P.L. Miller, T. Su, B. Yan, J. Yang, S. Guha, A. Madan, S.E. Shaheen, P.C. Taylor, R.T. Collins. *Appl. Phys. Lett.*, **102**, 133 101 (2013).
- [5] A.G. Kazanskii, Guanglin Kong, Xiangbo Zeng, Huiying Hao, Fengzhen Liu. *J. Non-Cryst. Sol.*, **354**, 2282 (2008).
- [6] R.A. Street. *Hydrogenated amorphous silicon* (Cambridge University Press, N.Y., 1991).
- [7] C. Delerue, M. Lannoo. *Nanostructures. Theory and Modelling* (Springer, Berlin, 2004).
- [8] A.S. Moskalenko, J. Berakdar, A.A. Prokofiev, I.N. Yassievich. *Phys. Rev. B*, **76** (8), 085 427 (2007).
- [9] K. Watanabe, M. Fujii, S. Hayashi. *J. Appl. Phys.*, **90** (9), 4761 (2001).
- [10] A. Belolipetskiy, O. Gusev, I. Yassievich. *J. Nanoelectron. Optoelectron.*, **9**, 750 (2014).
- [11] O. Maslova, A. Brezard-Oudot, M.E. Gueunier-Farret, J. Alvarez, W. Favre, D. Munoz, A.S. Gudovskikh, J.-P. Kleider. *Canadian J. Phys.*, **92**, 1–6 (2014).

Редактор К.В. Емцев